Supplementary Information

Insights on estimating urban CO_2 emissions using eddy-covariance flux measurements

Kyung-Eun Min[1*], Junphil Mun[1], Begie Perdigones[1], Soojin Lee[1], Kyung-Hwan Kwak[2]

[1]School of Earth Sciences and Environmental Engineering, Gwangju Institute of Science and Technology (GIST), Gwangju, 61005, Korea
[2]School of Natural Resources and Environmental Science, Kangwon National University, Chuncheon, 24341, Korea

Correspondence to: Kyung-Eun Min (kemin@gist.ac.kr)

S1. CFD results

The results of computational fluid dynamic modeling under the wind speed of 1.5 m s^{-1} from N, NE, E, SE, S, SW, W and NW directions are shown in Figure S1. The flux measuring system was installed on top of the helideck of the Gwangju city hall (shown in the middle) which is shown as red point. Color of the map represents wind speed in 1×1 m each grid.

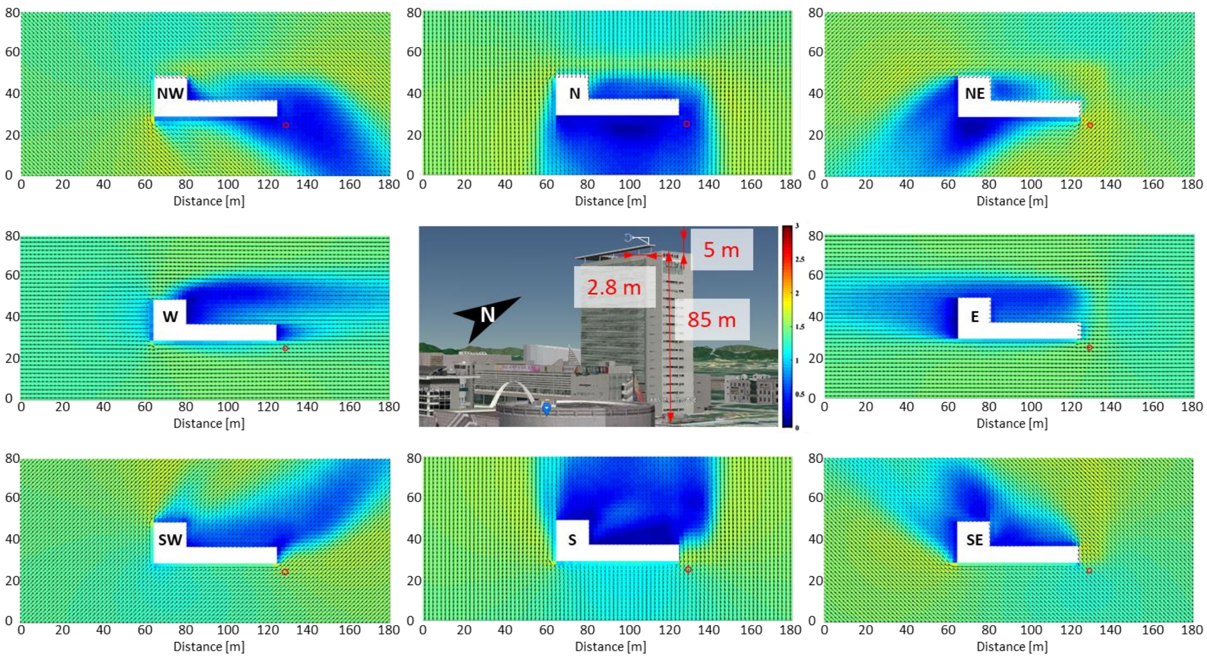

Figure S1. Computational fluid dynamic (CFD) modelling results with wind blowing from NW to W with 1.5 m s^{-1} shown in top left to middle left in clockwise direction with flux measuring system layout on the helideck. Colorbar represents the wind speed in each grid (1×1 m). Red circles on the CFD modelling result maps indicate the location of the measuring system. Image in the middle is provided by the geospatial information open platform, Vworld.

S2. Footprint analysis and atmospheric stability

Two different approaches- Kormann and Meixner (2001) model and Kljun (2004) model were used for the footprint analysis. Our analysis confined the footprint as 70% average of the total flux and the footprint results were drawn with five degree bins using the two different approaches (Figure 2a).

For Kormann and Meixner (2001), the relative flux (f) at distance x can be written as:

$$f = \frac{\xi^{\mu}}{\Gamma(\mu) \times x^{1+\mu}} \times \exp\left(-\frac{\xi}{x}\right), \tag{S1}$$

,where n is the eddy diffusion power law, m is exponent of the wind velocity power law and r is $2 + m - n$, μ is $(1 + m/r)$, and ξ stands for length scale which can be estimated as:

$$\xi = \frac{U z_m^r}{r^2 \kappa}, \tag{S2}$$

,where U is wind speed, z_m is measurement height and κ is Von Karman constant, 0.4.

For Kljun (2004), the NN% cumulative flux boundary ($X_{NN\%}$) is computed as:

$$X_{NN\%} = (x \times c - d) \times z_m \times (\sigma_w / u_*)^{-0.8}, \tag{S3}$$

, where z_m is measurement height, σ_w is standard deviation of vertical wind speed, u_* is friction velocity, x is the distance from the receptor which is function of b.

$$e^b \times b^{-b} \Gamma(b) \approx \frac{1}{A_c A_f}, \tag{S4}$$

, where constant parameters $A_c (4.28 \pm 0.13)$, and $A_f (= 0.18 \pm 0.01)$. c and d are functions of roughness length (z_0) as follows with parameters of B (3.42 ± 0.35) and A_d (1.68 ± 0.11).

$$c \approx A_c (B - ln z_0) \tag{S5}$$

$$d \approx A_d (B - ln z_0) \tag{S6}$$

Atmospheric stabilities are classified as unstable (ζ < -0.05), near nutral (-0.05 < ζ < 0.2) and stable (ζ > 0.2).

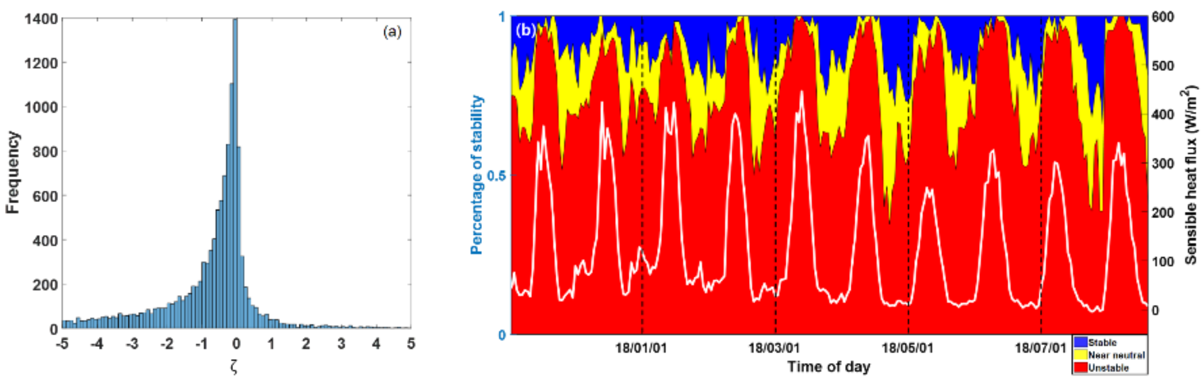

Figure S2. (a) Frequency histogram of length scale, ζ and (b) fractional distribution of monthly averaged diurnal pattern of atmospheric stability where blue, yellow and red represent unstable (ζ < -0.05), near neutral (-0.05 < ζ < 0.2) and stable (ζ > 0.2) condition, meanwhile, white line stands for sensible heat flux.

S3. Traffic information

Hourly averaged inferred traffic information was extracted from the ratio of in-situ traffic counts from the inbound and outbound of 6 highway tolls surrounding Gwangju (Gwangju, Donggwangju, Hakun, Songam, Seogwangsan and Donggwangsan, shown as red balloon), and occasional traffic survey on the adjacent cross roads in eastern and southern side of the city hall (Gyesu and Sangmu district, shown as yellow balloon), in hourly resolution as shown in Figure S3.

The diurnal patterns in different days of week are shown in Figure S4 with distinct bimodal patterns in morning and afternoon rush hours on weekday (Monday to Friday) and delays in morning peaks with broader afternoon peaks were observed for weekend (Saturday and Sunday). In general, relatively similar trends were observed for weekdays than weekend. Little difference in Monday with respect to the other weekdays were observed with slightly high in the morning (4:00 to 8:00) and low for the rest of the day (after 16:00). The ratios between sum of all highway tolls to Gyesu crossroad of each day are shown in Figure S4 e-g.

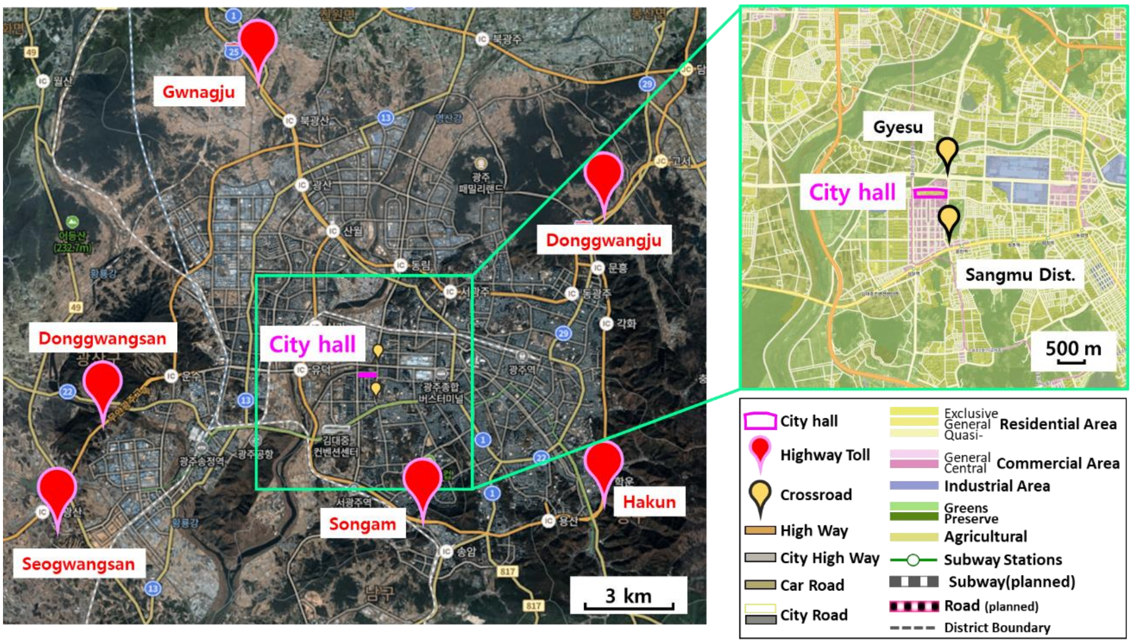

Figure S3. Traffic counts monitoring sites of highway tolls (red balloon) and crossroads (yellow balloon) within the 3 km fetch from Gwangju city hall (magenta polygon) on the top of the satellite image and land use (left and right figure). One should note that the land use map shown here only represents the major land use type for the case of multi-purpose land in 3D. © NAVER

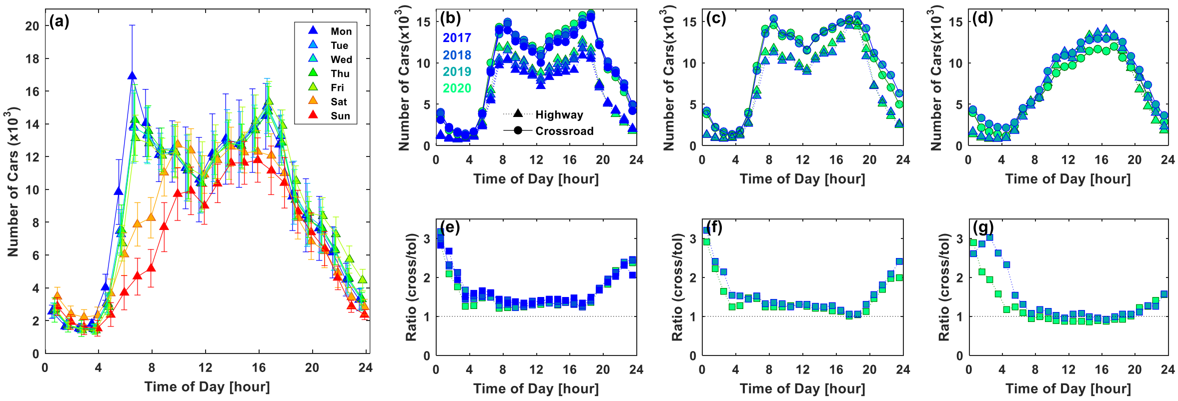

Figure S4. Diurnal patterns of traffic volume (a-d) in highway tolls (▲) and Gyesu crossroad (●) and their ratio (e-g, ■). Colors in (a) represent different days in a week and those in (b-g) indicate the years from 2017 to 2020. Crossroad

data collected by occasional survey for Tuesday to Thursday are available for the whole study period to 2020 (a and d), meanwhile, Friday (b and e) and Sunday (c and f) data are only accessible after 2019.

S4. HDD (heating degree days) estimation

HDD is calculated by multiplying the heating temperature and the number of days when the temperature was below 18 °C, assuming this tendency toward heating stops once the temperature reached 18 °C. Inferred HDD of September and October in 2018 with second order regression were used. The accumulated HDD in a year was 2330 °C.

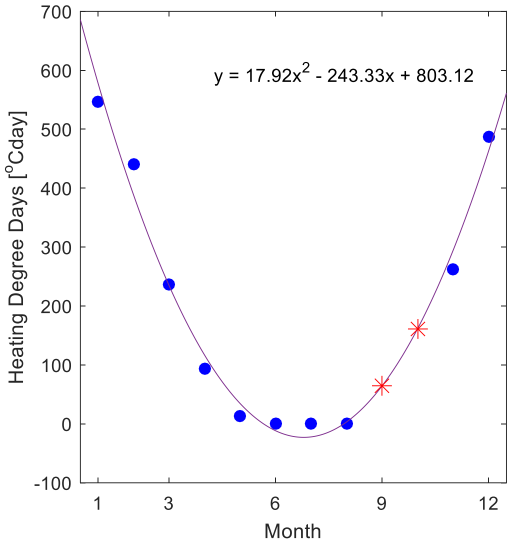

Figure S5. Calculated heating degree days (HDD) in each month with threshold temperature of 18 °C. Blue dots are the extracted HDD from the temperature measurements, red asterisks indicate the inferred HDD from the 2nd order polynomial regression curves (purple line)

S5. Monthly variations in CO_2 concentration and flux

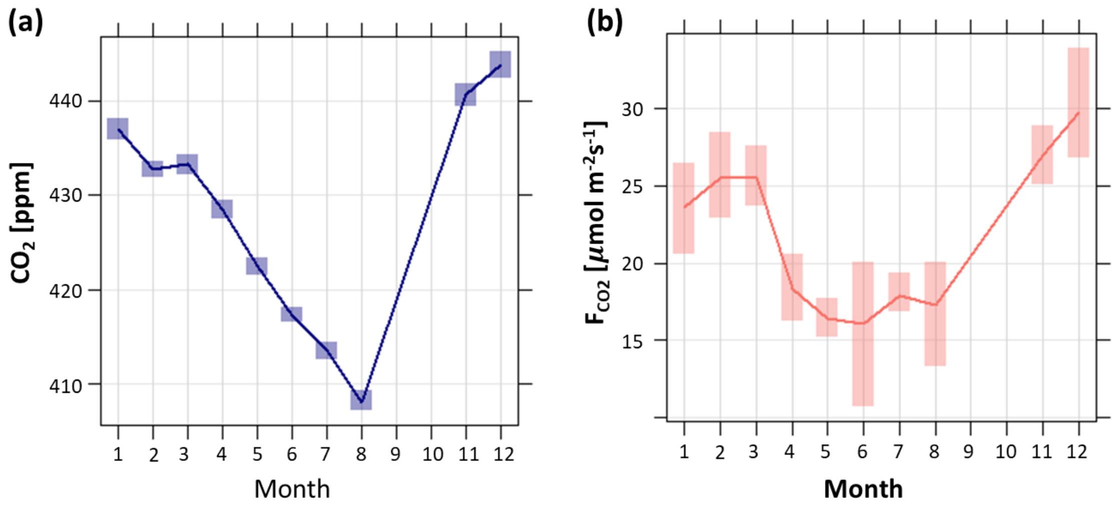

Figure S6. Monthly mean of (a) CO_2 mixing ratio and (b) flux measured from November 2017 to August 2018. Due to unfavourable weather condition in September, typhoon, the system had to be taken down.

S6. Traffic and CO_2 flux diurnal comparison

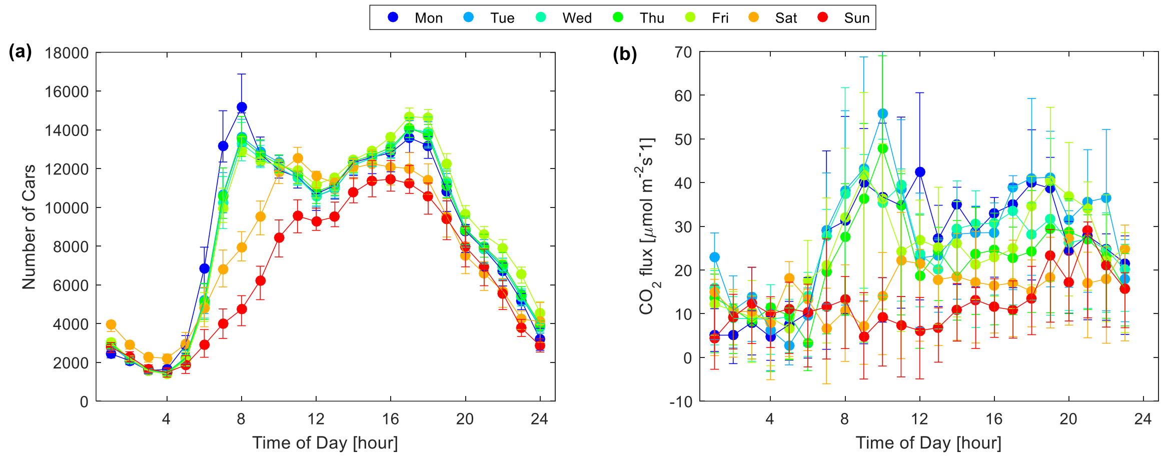

Figure S7. Diurnal pattern in each day of week for (a) inferred traffic counts and (b) CO_2 flux over the footprint ranges from 45° -225°. The whiskers represent interquartile range of distributions in each hour bin for whole study period.

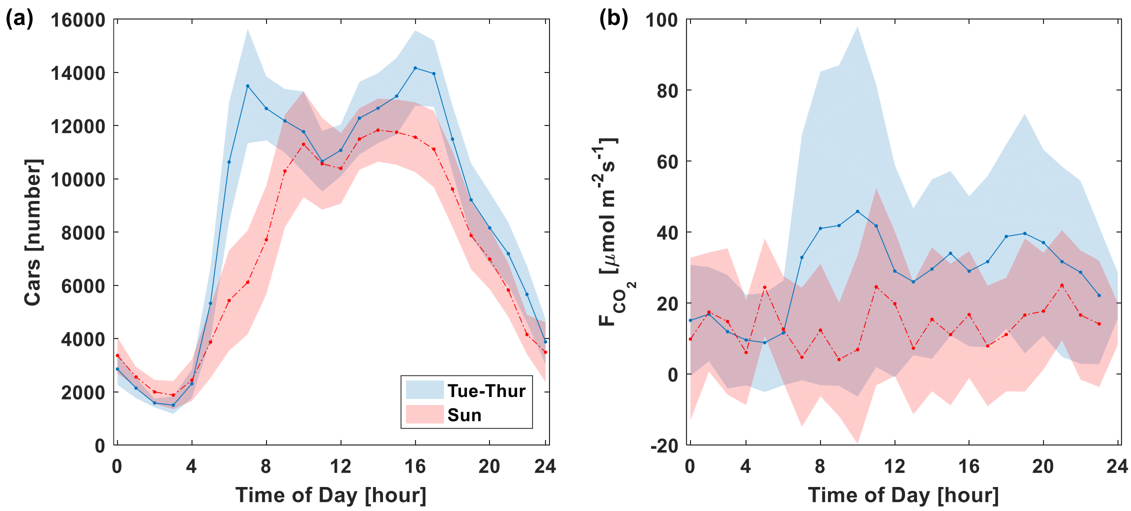

Figure S8. Diurnal pattern of weekday and weekend representative (Tuesday to Thursday in blue, Sunday in red) for (a) inferred traffic counts and (b) CO_2 flux over the footprint ranges from 45° - 100°.

S7. Yearly CO_2 emission estimation

Table S1. Summary of CO_2 flux, emission factors and year round emission for individual activity.

	Observed Flux		Traffic		Factory		Heat		Vegetation	
	value	unit	value	unit	value	unit	value	unit	value	unit
EF or flux	28.26	umol m^{-2} s^{-1}	0.017	umol m^{-2} s^{-1} car^{-1}	103.25	umol m^{-2} s^{-1}	2.41	umol m^{-2} s^{-1} °C^{-1}	-4.53	umol m^{-2} s^{-1}
Annual Operation (hr)	8760		8760		3856		8760		8760	
Area (km^2)	14.14		5.23		0.33		3.10		4.63	
Activity			4023	cars hr^{-1}			2330	°Cyr		
Flux (kg C m^{-2} yr^{-1})	**10.70**		**25.90**		**17.21**		**5.83**		**-1.72**	
Annual Emission (G g C yr^{-1})	151.35		135.53		5.72		18.04		-7.94	
Fraction	95%		85%		4%		11%		-5%	
Flux (kg CO_2 m^{-2} yr^{-1})	**39.22**		**94.92**		**63.08**		**21.35**		**-6.28**	
Annual Emission (G g CO_2 yr^{-1})	554.60		496.60		20.96		66.12		-29.08	